

# N92-22376

## SPACE DEBRIS CHARACTERIZATION IN SUPPORT OF A SATELLITE BREAKUP MODEL

Bryan H. Fortson, James E. Winter,  
and Firooz A. Allahdadi  
Space Kinetic Impact and Debris Branch, Phillips Laboratory  
Kirtland AFB, New Mexico 87117-6008

### ABSTRACT

The Space Kinetic Impact and Debris Branch has begun an ambitious program to construct a fully analytical model of the breakup of a satellite under hypervelocity impact. In order to provide empirical data with which to substantiate the model, debris from hypervelocity experiments conducted in a controlled laboratory environment has been characterized to provide information on its mass, velocity, and ballistic coefficient distributions. Data on the debris has been collected in one master data file, and a simple FORTRAN program allows users to describe the debris from any subset of these experiments that may be of interest to them. A statistical analysis has been performed, allowing users to determine the precision of the velocity measurements for the data. Attempts are being made to include and correlate other laboratory data, as well as those data obtained from the explosion or collision of spacecraft in low earth orbit.

### INTRODUCTION

Characterization of debris from hypervelocity impact events is an important prerequisite for analytical modelling of those events. One feature of a useful model would be its ability to predict the characteristics of the debris cloud produced by the impact, and this feature cannot be evaluated without a body of empirical data with which to compare the analytical predictions. The Space Kinetic Impact and Debris Branch (SKID) has conducted a debris characterization program, using hypervelocity impact debris produced in antisatellite experiments. Our approach includes some novel ideas from which the orbital debris community may benefit.

### WEIGHING AND CATEGORIZING OF DEBRIS

SKID has characterized debris from hypervelocity shots conducted at the Naval Research Laboratory (NRL) and at the University of Dayton Research Institute (UDRI). Most debris comes in plastic bags of two sizes, large and small. The large bags contain debris that has been swept from the floor of the impact chamber, and include a considerable amount of extraneous material. The smaller bags contain debris recovered from the inside of the impact target, and do not contain as much unwanted material.

The characterization begins with the sorting out of the metallic debris, from the non-metallic debris; this is done by hand. This provides another opportunity to remove extraneous material. The metallic debris is then weighed on the microbalance at Phillips Laboratory's metrology facility. This microbalance has an accuracy of 0.004 g. Debris particles with mass less than 10 times the accuracy of the scale are not weighed. The mass of the particle, as well as all pertinent information about the shot from which it came (shot number, impact angle, nominal projectile velocity, projectile material), is recorded in a master data file.

Some debris was collected in catcher material during the test, for the purpose of measuring its velocity. This debris is removed from the catcher material with tweezers, and the distance that it travelled into the catcher material is measured. This distance is used to determine the velocity at which the particle had travelled, using methods to be discussed later in this paper. The mass, velocity, and shot information are then included in the master data file.

## CALCULATION OF DISTRIBUTION CURVES

Calculation of mass distribution curves is performed by the FORTRAN-77 code DEBRIS.F. The program selects the data of interest to the user, and then generates a mass distribution plot, which is written to a file called DISTRIB.DAT. The data can be plotted in two ways. In the first approach, the dependent variable is mass, and the independent variable is the total number of debris particles larger than that mass. Such a plotting method is often used in the space debris community, for example, in References 1 and 2. In the second approach, the dependent variable is still mass, but the particles are separated into "bins." For example, a bin might contain all particles with mass between 0.1 g and 0.3 g. If 12 particles are found to lie in this range, the resulting data point would be (0.2, 12). This method of plotting is similar to the approach used by the debris hazard modeling computer program IMPACT<sup>(3)</sup>.

DEBRIS.F also fits a straight line and a parabola to the curve, and performs an F-test (as described in Reference 4) to determine if the higher-order fit is needed. The least-squares coefficients and the F-test results are written to a file called FITS.DAT. The source code can also generate velocity and ballistic coefficient distributions. DEBRIS.F, and the master data file DEBDAT, are installed on the CRAY-2 supercomputer at Kirtland AFB, whence they can be easily downloaded onto 5 $\frac{1}{4}$ " floppy disks.

It has been noted by McKnight<sup>(5)</sup> that a straight-line fit to a mass distribution does not make physical sense: if the line is extrapolated to the left, it is seen to imply the presence of an infinite number of infinitesimal particles. It makes more sense for the curve to have a "knee." Such a "knee" can be introduced with a bilinear least-squares fit, which has been derived as a part of this effort, and is available along with the linear and parabolic fits as part of the DEBRIS.F code.

Consider the situation shown in Figure 1: a bent straight line is to be fit to a set of data. The line is defined by four parameters: the intercept  $\beta_0$ , the two slopes  $\beta_1$  and  $\beta_2$ , and the x-coordinate of the break point,  $x_0$ . Consider the case in which  $x_0$  is given. A least-squares fit is obtained by minimizing the residual sum of squares  $SS(res)$ , given by

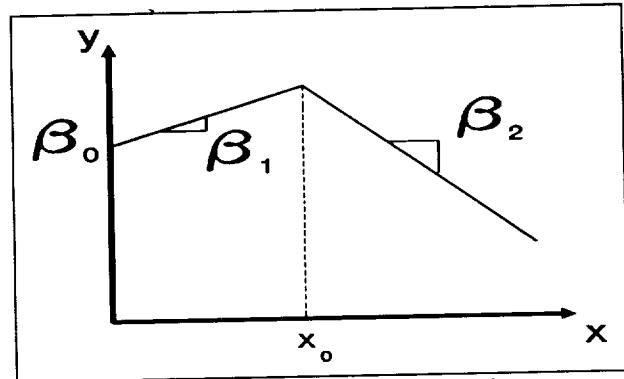


Figure 1. Definition of bilinear coefficients

$$SS(res) = \sum_{i=1}^{n_s} [y_i - (\beta_0 + \beta_1 x_i)]^2 + \sum_{i=n_s+1}^{n_T} [(y_i - \beta_0 - \beta_1 x_0) - \beta_2 (x_i - x_0)]^2 \quad (1)$$

where  $x < x_0$  for data points 1 through  $n_s$ , and  $n_T$  is the total number of data points. This is minimized by setting the partial derivatives of  $SS(res)$  with respect to the parameters equal to zero:

$$\frac{\partial SS(res)}{\partial \beta_0} = \frac{\partial SS(res)}{\partial \beta_1} = \frac{\partial SS(res)}{\partial \beta_2} = 0 \quad (2)$$

Substituting equation 1 into equations 2 leads to a system of three linear equations in three unknowns:

$$[\alpha] \begin{Bmatrix} \beta_0 \\ \beta_1 \\ \beta_2 \end{Bmatrix} = [\gamma] \quad (3)$$

where  $[\alpha]$  is a symmetric 3x3 matrix:

$$\alpha_{11} = n_T \quad (4)$$

$$\alpha_{12} = n_N x_0 + \sum_{i=1}^{n_s} x_i \quad (5)$$

$$\alpha_{13} = -n_N x_0 + \sum_{i=n_s+1}^{n_r} x_i \quad (6)$$

$$\alpha_{22} = n_N x_0^2 + \sum_{i=1}^{n_s} x_i^2 \quad (7)$$

$$\alpha_{23} = -n_N x_0^2 + x_0 \sum_{i=n_s+1}^{n_r} x_i \quad (8)$$

$$\alpha_{33} = \sum_{i=n_s+1}^{n_r} (x_i - x_0)^2 \quad (9)$$

the vector  $[\gamma]$  is defined as

$$[\gamma] = \left\{ \begin{array}{c} \sum_{i=1}^{n_s} y_i \\ \sum_{i=1}^{n_s} x_i y_i + x_0 \sum_{i=n_s+1}^{n_r} y_i \\ \sum_{i=n_s+1}^{n_r} (x_i - x_0) y_i \end{array} \right\} \quad (10)$$

and  $n_N$  is the number of data points for which  $x \geq x_0$ . This system can now be solved for  $\beta_0$ ,  $\beta_1$ , and  $\beta_2$ . Note that this solution requires a "guess" for  $x_0$ , but not for the  $y$ -value of the break point. The FORTRAN code DEBRIS.F performs 1001 bent-line fits to a given data set, using 1001 evenly-spaced guesses for  $x_0$ . The fit with the best correlation coefficient is retained.

This bilinear fit is particularly useful for applying the bilinear exponential model of Grady and Kipp<sup>[6]</sup>. Reference 6 proposes an equation of the form

$$y = A_1 e^{-B_1 x} + A_2 e^{-B_2 x} \quad (11)$$

This equation cannot be fit to a set of data using simple least-squares means; a more sophisticated, iterative approach is required. However, equation 11 approximates the bent-line fit if the  $x$ -axis is a linear scale, and the  $y$ -axis is a logarithmic scale. Thus, the bent-line fit can be applied to the model of Reference 6.

Figure 2 shows a mass distribution from DEBRIS.F, with the linear and parabolic fits employed. Data from all shots that were characterized was combined into one file, which is plotted here. The  $x$ -coordinate is a chosen mass  $M$ . The  $y$ -coordinate is the number of particles observed to have a mass greater than  $M$ . The F-test performed by the program indicates that

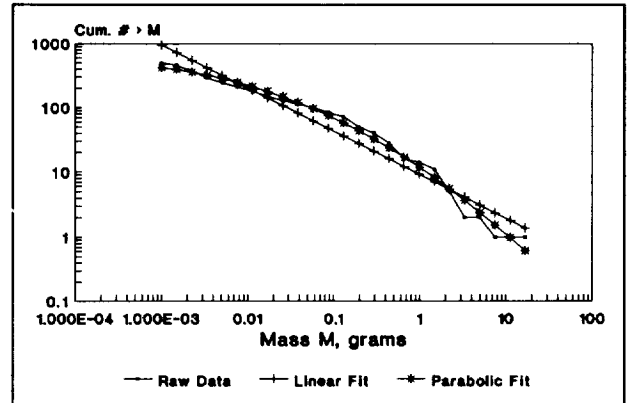


Figure 2. Mass distribution curve.

the accuracy gained by using the parabolic fit, as opposed to the linear fit, is statistically significant in this case.

Figure 3 shows the same data, separated into bins of uniform width on a logarithmic scale. (Bins can also be of uniform width on a linear scale.) The  $x$ -coordinate of each data point corresponds to the center of the bin. Linear and parabolic fits are also available with this type of plot.

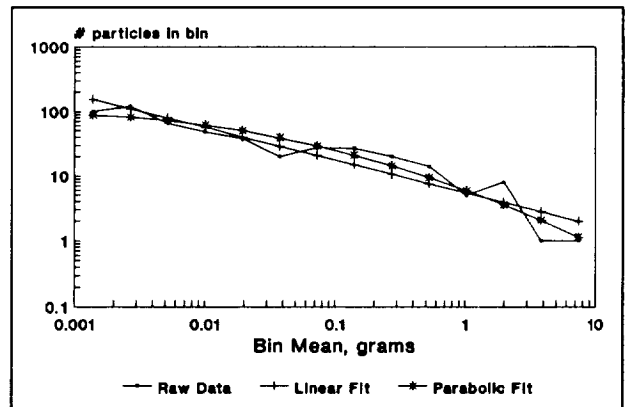


Figure 3. Sample plot with data separated into bins

Figure 4 shows the same data, plotted with the bilinear fit routine. At first glance, the fit does not appear to be very good. However, a closer look shows that the linear scale on the  $x$ -axis leads to a

concentration of data points near the left-hand side of the graph. Once these points are recognized, the fit is seen to be quite good.

Figure 4 also shows that, when the distribution data is plotted with a linear x-axis, the resulting curve is almost vertical at low values of  $x$ . For some test data, this steepness caused numerical stability problems in the bilinear fit routine, which resulted in negative values of  $R^2$  for some or all of the trial fits. These stability problems were decreased, but not eliminated, by restricting the range of the trial values of  $x_0$ . The problem was solved by implementing a completely pivoted Gaussian elimination routine to solve equation 3. DEBRIS.F had previously solved equation 3 with an unpivoted Gaussian elimination.

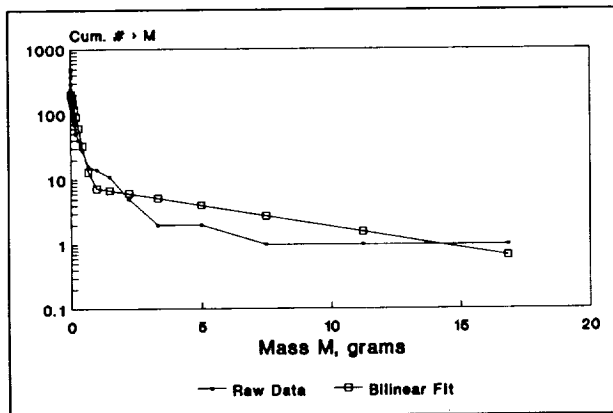


Figure 4. Mass distribution plot with bilinear fit.

Figures 5 and 6 show individual plots for all tests, using the plotting formats of Figures 2 and 3. Figure 6 used a linear vertical axis, due to the presence of some zero values in the data. This format also emphasizes the differences in the data from the various tests. The most interesting result is the considerable variation among the curves shown in these two figures. These shots are actually quite similar; yet, their debris distributions are quite different. It should be noted that, while no debris particles of mass less than 0.04 g were weighed, this limitation would not change the values given in Figures 5 and 6; it would merely allow the curves to be extended to the left. Thus, the variability shown in these figures is real.

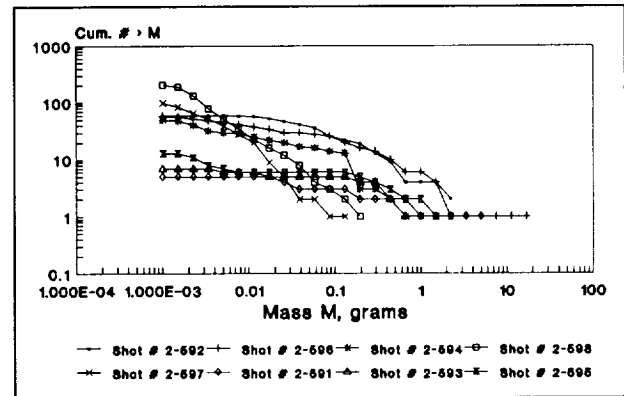


Figure 5. Mass distribution plots for individual tests.

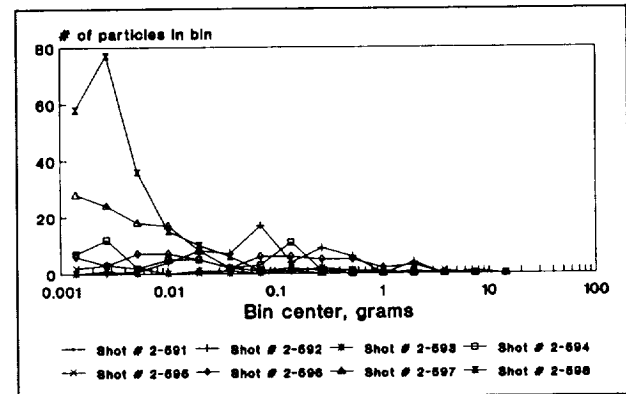


Figure 6. Individual mass distribution plots, using bin format.

The flexibility of this approach would also be useful in studies such as Reference 2. McKnight and Brechin determined the linear fit coefficients for the mass distributions of several impact events, and fit a curve to these coefficients in an effort to create a master equation to describe the mass distributions of a wide range of impact events. Using the SKID method of cataloging the debris, a large body of data could be built up and easily analyzed. Effects of varying parameters (such as projectile mass, projectile velocity, projectile material, etcetera) on the linear or parabolic fit parameters could be observed.

#### STATISTICAL ANALYSIS OF VELOCITY MEASUREMENTS

Velocity measurements are taken using the results of Malick's empirical study<sup>[7]</sup>. Malick fired test projectiles of four different materials at wallboard, using a

range of known velocities, masses, impact angles (see Figure 7), and presented particle areas.

Malick then fit a curve to his data. The

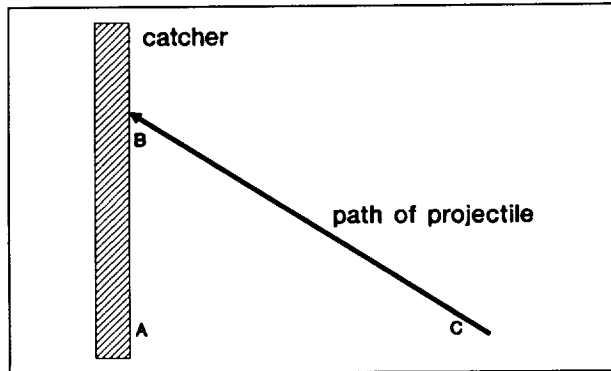


Figure 7. Definition of impact angle  $\theta$  ( $\triangle ABC$ ).

resulting equation was:

$$V = \frac{1537 f_v t^{0.8091}}{m^{0.3336} (\cos \theta)^{0.5419}} \quad (12)$$

where  $V$  is the particle velocity in ft/sec,  $f_v$  is a function of the projectile density,  $t$  is the thickness of particle board penetrated, in inches,  $m$  is the weight of the particle, in grains, and  $\theta$  is the impact angle. The multiple correlation coefficient for the fit of this curve to the data is 0.88. Equation (12) applies only to the case of approximately cylindrical projectiles, for which

$$A \approx cm^{2/3} \quad (13)$$

where  $A$  is the average presented area of the particle, and  $c$  is a constant.

Figure 8 shows the results of fitting a power-law curve to Malick's data for  $f_v$  as a function of density. The resulting curve is:

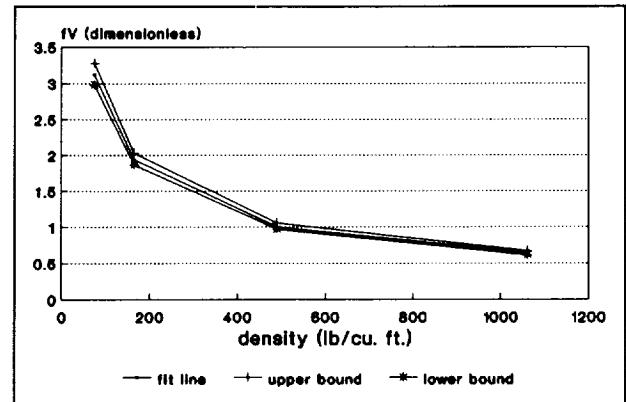


Figure 8. Power-law fit to Malick's data

$$f_v = \frac{41.2}{\rho^{0.6}} \quad (13)$$

where  $\rho$  is the projectile density in lb/ft<sup>3</sup>. This curve fits the common logarithms of Malick's data with a correlation coefficient of  $R^2=0.9996$ . Figure 8 shows a 95% prediction confidence interval drawn about this curve, illustrating the reliability of interpolations of  $f_v$  made on the basis of it. Incorporating equation (13) into equation (12) gives

$$V = \frac{6.332 \times 10^4 t^{0.8091}}{m^{0.3336} \rho^{0.6} (\cos \theta)^{0.5419}} \quad (14)$$

It is important to know the reliability of velocity measurements made with Malick's equation. A prediction confidence interval for these measurements can be constructed, using the approach found in Bancroft and Han.<sup>181</sup>

A multiple linear regression used to obtain equation (14) would begin with an equation of the form

$$\begin{aligned} \log V'_i &= b_0 + b_1 \log \rho_i \\ &+ b_2 \log t_i + b_3 \log m_i \\ &+ b_4 \log (\cos \theta_i) \end{aligned} \quad (15)$$

where  $V'_i$  is the least-squares approximation to the actual velocity  $V_i$ . For convenience, rewrite equation (15) as

$$\begin{aligned} \log V'_i &= b_0 + b_1 x_{1i} + b_2 x_{2i} \\ &+ b_3 x_{3i} + b_4 x_{4i} \end{aligned} \quad (16)$$

where the following abbreviations are used:

$$\log \rho = x_1 \quad (17)$$

$$\log t = x_2 \quad (18)$$

$$\log m = x_3 \quad (19)$$

$$\log(\cos \theta) = x_4 \quad (20)$$

Now, define the matrix [C] to be the inverse of the matrix [D], for which

$$D_{kl} = \sum_{i=1}^n x_{(k-1)I} x_{(l-1)I} \quad (21)$$

where all summations are taken over all n data points  $(V_i, x_{1i}, x_{2i}, x_{3i}, x_{4i})$ , and  $x_0$  is defined as 1. Furthermore, define the quantity  $S^2$ :

$$S^2 = \frac{1}{n-p} \sum_{i=1}^n (\log V_i - \log V'_i)^2 \quad (22)$$

where p is the number of degrees of freedom in the model. For this case,  $p=5$ ; there are four coefficients in the regression equation, plus one constant.  $S^2$  is an unbiased estimator of the variance of the errors of the data relative to the least-squares fit, assuming those errors to be normally distributed. Under this assumption, a  $100(1-\alpha)\%$  confidence interval for  $V_i$  is given by

$$V'_i \pm t_{(\alpha/2, n-p)} S \sqrt{\{X\}^T [C] \{X\}} \quad (23)$$

where

$$\{X\} = \{1 \ x_1 \ x_2 \ x_3 \ x_4\}^T \quad (24)$$

and  $t_{(\alpha/2, n-p)}$  is the  $100(1-\alpha/2)\%$  point of Student's t-distribution, with n-p degrees of freedom. Tables of this distribution are readily available in most probability texts. A  $100(1-\alpha)\%$  prediction interval is given by

$$V'_i \pm t_{(\alpha/2, n-p)} S \sqrt{1 + \{X\}^T [C] \{X\}} \quad (25)$$

Thus, it is necessary to calculate the estimator  $S^2$  and the matrix [C] from Malick's original data, after which the desired confidence intervals can be calculated by plugging the vector {X} into the appropriate equation.

Converting equation (14) to the MKS system gives

where V is now measured in m/sec,  $\rho$  is in  $\text{kg/m}^3$ , t is in meters, and m is in kilo-

$$V = \frac{1.108 \times 10^3 t^{0.8091}}{m^{0.3336} \rho^{0.6} (\cos \theta)^{0.5419}} \quad (26)$$

grams. With all data available from Reference 7 converted to MKS, the matrix [C] was calculated, and, using equation (26) as the fit to the data, the value of S was determined to be

$$S = 0.144 \quad (27)$$

Two facts about the data of Reference 7 are worth noting. First, the majority of shots were fired at impact angles of zero degrees, leaving relatively little information on the variation of V with  $\theta$ . This is reflected in the large value of the coefficient  $C_{55}$  in the matrix [C], which indicates that the width of the confidence interval is very sensitive to  $\theta$ . Second, the highest impact velocity recorded for valid data is about 9000 ft/sec, or about 2.7 km/sec. Malick performed some shots at higher speeds, but considered the resulting data invalid because of excessive breakup or deformation of the projectiles. Thus, the average velocity for Malick's shots is probably 1.0 - 1.5 km/sec. Figure 9, a schematic of the confidence and prediction bands about a simple least-squares straight-line fit, shows why this is important. The confidence band, which is described by equation 23, is tightest at the mean x-value of the data. Its width varies as the square of the distance from this point along the x-axis. Because of the linear nature of the fit, one can make a similar statement regarding the variation with distance from the mean y-value of the data. For the same confidence level, the prediction band, described by equation 25, behaves in a similar manner, but is much wider. The geometrical interpretation is more complex for a multiple regression. However, one can say that Malick's fit is probably most accurate for velocities of approxi-

mately 1.0 - 1.5 km/sec, and that the accuracy of this method decays for values significantly outside of this range. Thus, it is important to have a quanti-

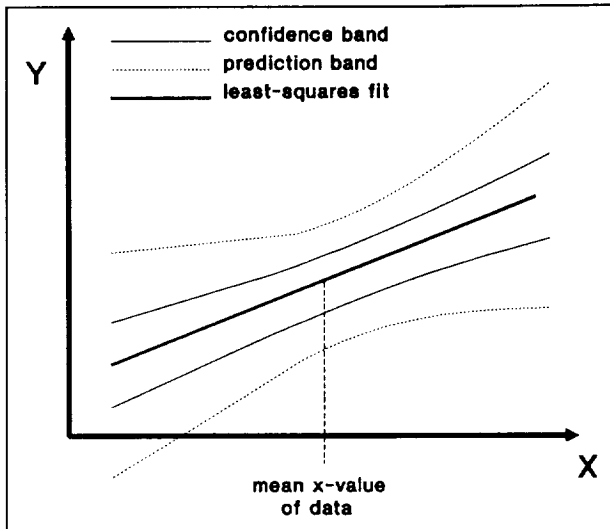


Figure 7. Schematic of confidence and prediction intervals.

tative measure of the accuracy of the velocity values thus obtained.

As an example, consider the first data point given in Reference 7. The velocity is seen to be 966 ft/sec, or 294 m/sec. Converting the mass, density, and thickness to the MKS system, and using equation (25), Malick's curve fit is seen to indicate a velocity of 493 m/sec for this projectile. This illustrates a difficulty resulting from fitting a curve to the logarithm of the velocity data: Malick's velocity estimate is in error by almost 70%, but this results from a creditable 9% error in estimating the logarithm of the velocity.

Using the definitions of equations (17) - (20), and substituting into equation (23), a 90% confidence interval for this data point is found to be

$$442\text{ m/sec} \leq V \leq 542\text{ m/sec} \quad (28)$$

However, a 90% prediction interval for this same projectile, calculated using equation (25), would be much larger:

$$281\text{ m/sec} \leq V \leq 853\text{ m/sec} \quad (29)$$

## CONCLUSION

Since the appropriate statistical parameters have been calculated, one can now use equations (23) and (25) to determine the accuracy of any velocity prediction made using Malick's method.

The method of creating debris characterization plots is very versatile. The data file collected for this program can be added to at any time, and the computer code that reads it is simple and easily modified. This flexible approach will allow this database to be expanded and restudied as new issues arise in debris characterization.

## ACKNOWLEDGEMENTS

This work was supported by the Electronic Systems Division of the Air Force Systems Command, under the management of Ms. Gail Collamore, ESD/SRA.

## REFERENCES

1. Maclay, T., and Ilinga, M., "Analysis of Shot CU-5272 Fragments," COLORADO CENTER FOR ASTRODYNAMICS RESEARCH IN TERNAL RESEARCH REPORT NO. 153-6416, University of Colorado at Boulder, June, 1990.
2. McKnight, Darren, and Brechin, Christopher, "Debris Creation Via Hypervelocity Impact," PAPER NO. AIAA-90-0084, American Institute of Aeronautics and Astronautics, Washington, DC, 1990.
3. Sorge, M.E., "Space Debris Hazard Software: Program IMPACT Version 1.0 B," AEROSPACE REPORT NO. TOR-0091(6909-04)-1, The Aerospace Corporation, El Segundo, CA, January, 1991.
4. Miller, Irwin, and Freund, John E., PROBABILITY AND STATISTICS FOR ENGINEERS, Prentice-Hall, Englewood Cliffs, New Jersey, 1977. Pp. 319-320.
5. McKnight, Darren, private communication, January 1991.
6. Grady, D.E., and Kipp, M.E., "Geometric Statistics and Dynamic Fragmentation," JOURNAL OF APPLIED PHYSICS, vol. 58, no. 3, pp. 1210-1222.

7. Malick, D., "The Calibration of Wall-board for the Determination of Particle Speed," Ballistic Analysis Laboratory TECHNICAL REPORT NO. 61, May, 1966, The Johns Hopkins University.

8. Bancroft, T.A., and Han, Chien-Pai, STATISTICAL THEORY AND INFERENCE IN RESEARCH, Marcel Dekker, Inc., New York, New York, 1981. Pp. 277-289.